Binding of Ochratoxin A to Human Serum Albumin Stabilized by a Protein−Ligand Ion Pair

Jennifer L. Perry,[‡] Trine Christensen,[‡] Michael R. Goldsmith,[‡] Eric J. Toone,[‡,§] David N. Beratan,[‡,§] and John D. Simon*[,‡,§]

Department of Chemistry, Duke University, Durham, North Carolina 27708, and Department of Biochemistry, Duke University Medical Center, Durham, North Carolina 27710

Received: March 27, 2003; In Final Form: June 4, 2003

Ochratoxin A (OTA), a fungal metabolite of strains of *Penicillium* and *Aspergillus*, binds in its dianion form to Sudlow site I of human serum albumin (HSA) with high affinity. In this study, isothermal calorimetry (ITC) is used to study the binding of OTA and its *O*-methyl derivative (MOA). Calculations of the equilibrium geometry of the monoanion and dianion of OTA reveal only small structural changes among the lowest energy conformers. The ITC data show the binding of MOA, which lacks the phenolic proton of OTA, is accompanied by the uptake of a proton from the surrounding solvent. At pH 7.13, the binding of OTA is accompanied by uptake of 0.43 ± 0.15 protons from the solvent. At this pH, the monoanion (0.54) and dianion (0.46) forms of OTA are both present in solution. However, the pK_a of the phenolic group of OTA decreases by more than three units upon protein binding, and so all available OTA is bound to the protein as the dianion. To account for the ITC data, a model is proposed in which the proton is provided by the phenolic moiety of OTA in the case of initial binding of the monoanion, and a proton is taken up from the surrounding solvent for initial binding of the dianion. The binding constant of MOA is 2 orders of magnitude smaller than that of OTA, indicating the ion pair between the phenoxide group of OTA and the protonated amino acid is a major contributor to the high binding affinity of OTA to HSA. To identify the specific amino acid involved, the binding of OTA to bovine, rat, and porcine serum albumins was examined. Deprotonation of the monoanion of OTA occurred upon binding to all species. Assuming the amino acid is conserved between species and taking into account crystal structures of ligands bound to site I of HSA and their ability to displace OTA from HSA, either R218 or R257 is involved in the ion pairing with OTA. These two amino acids sit across the binding cavity from one other in site I.

Introduction

Ochratoxin A (OTA, Chart 1) is a fungal metabolite produced by *Aspergillus* and *Penicillium* species.[1,2] The prevalence of OTA in improperly stored foods[3−5] has raised human health concerns as OTA has been detected in human plasma globally.[6−9] At concentrations present during normal dietary intake (nanomolar range), OTA is believed to generate chronic changes in renal function.[10] OTA exposure has led to disruption of cellular pH and Ca^{2+} homeostasis in proximal tubule cells.[11,12] Furthermore, increases in pH values have been reported in the nephron collecting duct and the descending and ascending vasa recta blood after incubation with OTA, which are attributed to OTA impairment of HCO_3^- reabsorption.[13] Although OTA interacts with transporters on both basolateral and apical membranes, proposed mechanisms suggest the entry of OTA into renal cells occurs on the apical membrane.[6] Na^+ independent organic anion and proton-dipeptide transporters along the apical membrane that transport OTA in MDCK cells are believed to be responsible.[14] In addition, an unidentified pH dependent transport mechanism is believed to occur, as known inhibitors failed to block all OTA uptake.[15]

CHART 1: Molecular Structures of the Monoanions of OTA and MOA

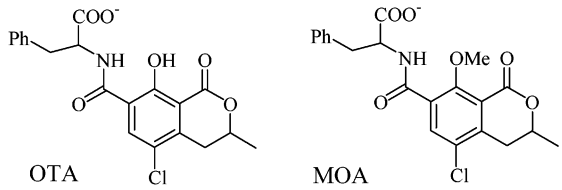

Within the body, OTA exists primarily as a complex with serum albumin, which is responsible for the transport of the toxin. Binding to albumin has been identified for several species and binding constants increase in the following order 4.0×10^4 M^{-1} (rat)[16,17] > 5.1×10^4 M^{-1} (chicken)[16,17] > 7.1×10^4 M^{-1} (porcine)[16,17] > 3.2×10^5 M^{-1} (bovine)[18] > 5.2×10^6 M^{-1} (human).[19] The sequence homology (see Figure 5) between these serum albumins indicates a large number of conserved amino acids.

OTA possesses two ionizable moieties and the reported pK_as of the carboxyl and phenolic moieties on OTA range from 4.2 to 4.4 and 7.0−7.3, respectively, in aqueous solutions.[18,20,21] Therefore, the monoanion (OTA^-) and dianion (OTA^{2-}) forms of OTA are both present to an appreciable extent at physiological pH. The *O*-methyl ester of OTA (MOA) (see Chart 1) exists at physiological pH as a monoanion (MOA^-). Methylation at the site of the hydroxyl moiety of OTA prevents dianion formation.

* Correspondence should be sent to: John D. Simon, Department of Chemistry, Duke University, Durham, NC, 27708-0346; jsimon@duke.edu; 919-660-1508 (p); 919-660-1605 (f).
‡ Department of Chemistry.
§ Department of Biochemistry.

10.1021/jp034783x CCC: $25.00
Published on Web 07/03/2003

The binding of both OTA and MOA to human serum albumin (HSA) has been studied. Experimental data support the conclusion that an OTA binding site exists in domain IIA (site I) and in domain III (site II) with binding constants of 5.2×10^6 and 1.0×10^5 M^{-1}, respectively.[22] When bound to HSA in site I (its highest affinity site), the pK_a of the hydroxyl moiety of OTA shifts to 3.9.[19] Thus, at or near physiological pH, the solution contains an equilibrium mixture between OTA^- and OTA^{2-}, but only OTA^{2-} is observed bound to the protein. Under conditions where [OTA] < [HSA], essentially complete binding is observed. MOA binds to HSA with a binding constant of 3.0×10^4 M^{-1}.[23] Displacement with 2,3,5-triidobenzoate (TIB) in HSA and binding to recombinant domains of the protein indicate the location of the binding site for MOA is within site I, similar to OTA.[23]

Whether the proton liberated upon deprotonation of OTA^- to OTA^{2-} remains in the protein or is released into solution has not been resolved. In this work, isothermal calorimetry (ITC) is used to obtain thermodynamic information on the binding of OTA and MOA to HSA. By examining the binding in a series of buffer solutions, the role of proton exchange between OTA, the protein, and the solvent can be addressed.

Experimental Section

Calculations. Conformational analyses of OTA were computed using MacroModel 7.0 (Schrodinger Inc.) with the MMFF force-field and the water GB/SA solvation model.

Materials. Ochratoxin A (OTA) was purchased from Sigma and was used without further purification. MOA was synthesized as described previously.[2,24] Aqueous solutions were prepared by dissolving OTA or MOA in methanol (Fisher), evaporating the solvent, and adding to the buffer solution. HSA was dissolved into the buffer solution. Phosphate (44.05 mM), Tris, and MOPs (all from Fisher) buffers were prepared from corresponding acidic and basic components dissolved in HPLC Water (Fisher) to reach a final pH of 7.13. The ionic strength was adjusted to 0.1 by adding NaCl. Fatty acid free HSA, bovine serum albumin (BSA), rat serum albumin (RSA), and porcine serum albumin (PSA) (Sigma-Aldrich) were utilized.

ITC. Protein and ligand concentrations were determined by their respective molar absorptivities. Absorption spectra were recorded with a diode-array spectrometer (Hewlett-Packard 8452A). Thermodynamic data were collected on a VP-ITC titration microcalorimeter (MicroCal, Inc.); details of instruments and data reduction have been reported previously.[25] Concentration ratios between ligand and protein were [MOA]/[HSA] ≥ 10 and [OTA]/[HSA] ≥ 20. The c value ($c = K_a$[protein], where K_a is the binding affinity)[26] that describes the concentration range between MOA and HSA was ~4.5 whereas that between OTA and HSA was ~10. Ligand and reference buffer solutions were degassed under vacuum prior to titration experiments. After equilibrium at 25 °C was reached, each ligand was injected into a 1.4346 mL protein solution using the following parameters: 25−30 14 s injections, 6−7 μL per injection, 5 min intervals. MicroCal Origin software (Version 5.0) was utilized to fit ITC titration curves. Values for ΔH_{buffer} utilized in the ΔH_{app} as a function of ΔH_{buffer} plots were obtained from ref 27.

Fluorescence. Excitation spectra were collected via a Fluorolog 3 fluorometer (Jobin-Yvon-Horiba) to examine protolytic equilibrium of OTA in the presence of HSA, BSA, RSA, and PSA. A 50 mM phosphate buffer, pH 7.20 was utilized. Solutions were incubated for 30 min prior to the measurement of excitation spectra in the presence of air at +25 °C.

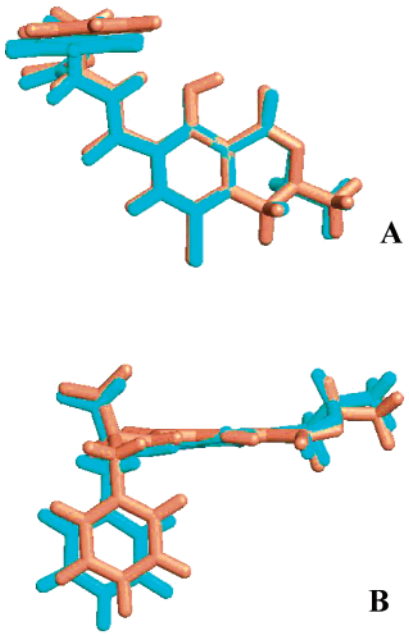

Figure 1. Lowest energy conformations of OTA^- (red) and OTA^{2-} (blue) in the top (A) and side (B) views.

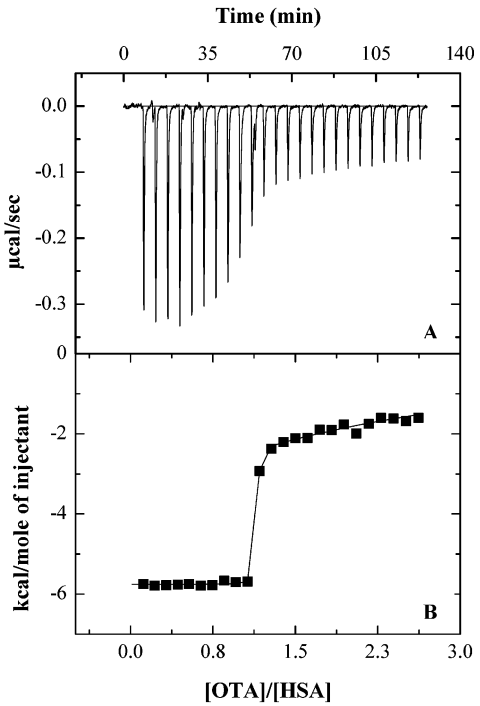

Figure 2. ITC titration of OTA with HSA in 44.05 mM Tris buffer, pH 7.13 and $I = 0.1$: (A) differential power recorded in the experiment; (B) integration of areas under peaks corresponding to the amount of heat released upon the addition of OTA to HSA as a function of the molar ratio [OTA]/[HSA].

Results

Calculations. Parts A and B of Figure 1 overlap the minimum energy conformers of the monoanion and dianion of OTA. Slight conformational changes occur between OTA^- and OTA^{2-}. Small shifts in the relative orientation of the phenyl ring and to a lesser extent the lactone ring are apparent.

ITC. ITC titration curves were collected for both ligands binding to HSA. Figure 2 shows one of the ITC titration curves for OTA and HSA in Tris buffer (top) and the resulting two-site fit of the integrated differential power signal with respect

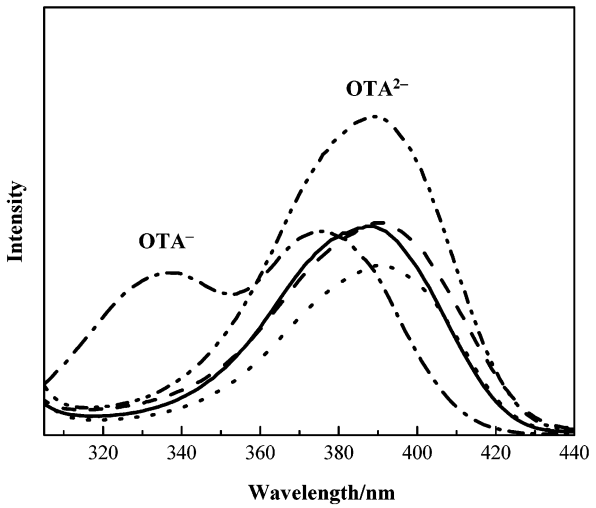

Figure 3. Fluorescence excitation spectra of 1 μM OTA (dash−dot) in the presence of 100 μM RSA (solid), PSA (dash−dot-dot), BSA (dot), and HSA (dash) in a 50 mM phosphate buffer pH 7.20 following emission at 450 nm.

TABLE 1: ITC Determinations of ΔH_{app} (kcal/mol) for 44.05 mM Buffers pH 7.13 with $I = 0.1$ at 25 °C

buffer	ΔH_{app} (kcal/mol) MOA/HSA	ΔH_{app} (kcal/mol) OTA/HSA
Tris	0.3	−5.76
MOPs	−2.2	−6.26
phosphate	−11.2	−8.71

to time (bottom). Table 1 lists the total heat released, ΔH_{app}, determined from the ITC titration curves for each buffer solution examined for both MOA and OTA binding to HSA.

Binding of OTA to Albumins. Figure 3 shows the fluorescence excitation spectra of OTA bound to various serum albumins. In the absence of albumin, two peaks are observed in the emission excitation spectrum, reflecting OTA^- and OTA^{2-}, respectively. Upon binding to the albumins studied, only the dianion peak is observed in the emission excitation spectrum, unambiguously demonstrating that the toxin is bound predominantly as the dianion. The maximum of the excitation spectrum for the OTA dianion differs slightly among the albumins studied. The OTA dianion maximum is 387, 388, 389, and 390 nm for RSA, PSA, HSA, and BSA, respectively. We previously noted the extent of the bathochromatic shift present for OTA^{2-} is influenced by the presence of domain I of HSA.[22] Thus differences in amino acid composition among the serum albumins and the resulting effect on the binding cavity may explain slight shifts present in the OTA^{2-} maximum.

Discussion

Proton Uptake by HSA upon Ligand Binding. The total heat, ΔH_{app}, measured by ITC reflects the heat of dilution of the ligand into the buffer and enthalpic changes associated with the binding of the ligand to the protein. Specific to the current study, ΔH_{app} will also contain contributions for any changes in the protonation state of the ligand or protein upon binding as well as any exchange of those proton(s) with the buffer. Protons that are exchanged with the buffered environment contribute to the respective buffer ionization enthalpy of the buffer, ΔH_{buffer}. In that case, ΔH_{app} depends on ΔH_{buffer} and the binding enthalpy, ΔH_{bind}. For a series of buffers at constant pH and ionic strength, but different heats of ionization, ΔH_{app} can be

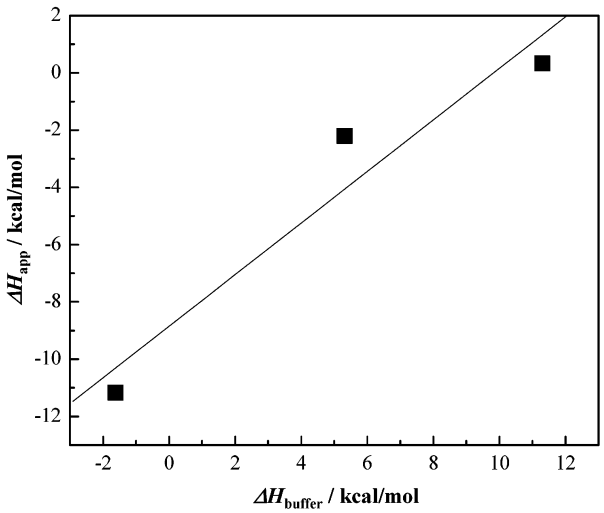

Figure 4. Plot of ΔH_{app} as a function of ΔH_{buffer} from the ITC curves of MOA binding to HSA. The resulting equation of the best-fit line is $y = 0.90x - 8.8$ with $R^2 = 0.92$.

expressed as follows:[26]

$$\Delta H_{app} = \Delta H_{bind} + n_H{}^+ \Delta H_{buffer} \quad (1)$$

where $n_H{}^+$ is the number of protons released to (negative) or taken up from (positive) the buffer upon ligand binding. The value of $n_H{}^+$ can be found from the slope of a plot of ΔH_{app} as a function of ΔH_{buffer}; the intercept is ΔH_{bind}.

First, consider the binding of MOA to HSA. Both MOA and OTA can be displaced from HSA using the ligand TIB, suggesting that both MOA and OTA occupy the same binding site within the protein. This conclusion is also consistent with binding studies of the two ligands to recombinant domains of HSA.[23] The plot in Figure 4 shows ΔH_{app} as a function of ΔH_{buffer}. A fit to the experimental data gives a slope of $n_H{}^+ = 0.90 \pm 0.25$, indicating the binding of MOA to HSA is accompanied by the uptake of approximately one proton by the protein. The intercept of the line gives $\Delta H_{bind} = -8.8 \pm 1.8$ kcal mol^{-1}.

The binding of OTA to HSA is more complicated than MOA because, as discussed above, under physiological conditions OTA^- and OTA^{2-} are both present to an appreciable extent. The experiment could, in principle, be simplified by working at a pH where only the OTA dianion is present. However, HSA undergoes several pH transitions. At physiological pHs, HSA is in its normal (N) conformation. However, as pH increases (pH > 8) a decrease in helical content occurs (commonly called the basic (B) form). Likewise, low pHs (pH < 4) and (pH < 3.5) prompt the formation of the fast (F) and extended (E) conformations, respectively.[28] Ligand binding to HSA depends on the protein conformation. Although warfarin shows higher affinity binding in the B form,[29] OTA binds with much lower affinity than in the N form.[19] Therefore, it is important to examine the binding at physiological pH and subsequent data analysis must consider the equilibrium between OTA^- and OTA^{2-}.

In the buffers utilized (pH 7.13), the mole fractions of OTA^- and OTA^{2-} are 0.54 (±0.02) and 0.46 (±0.02), respectively. For the concentrations used in the calorimetry experiments, essentially complete binding of the toxin occurs. Because the pK_a of the phenolic group decreases by more than three units upon protein binding, only OTA^{2-} is bound. Therefore, OTA^- present in solution must be deprotonated upon binding. The

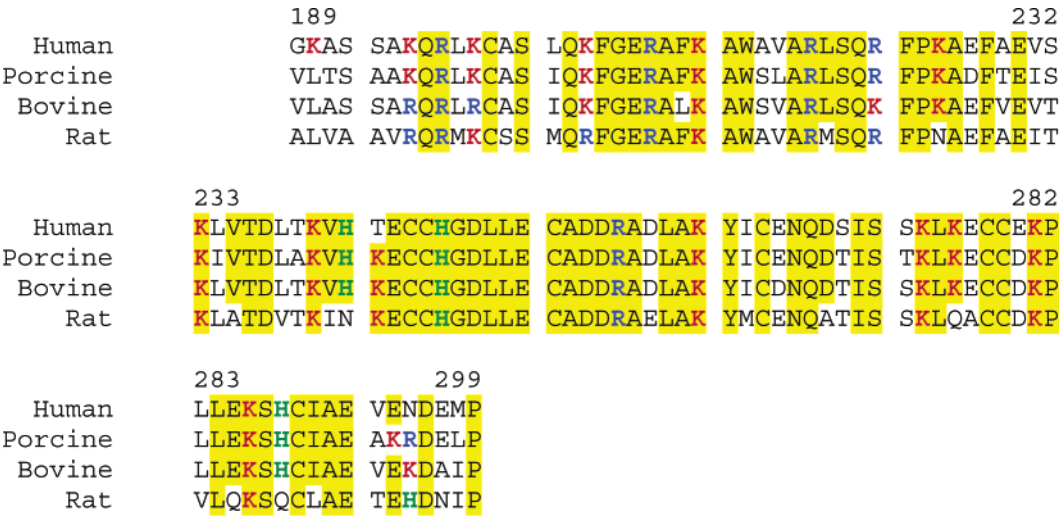

Figure 5. Sequence analysis of subdomain IIA of serum albumins. Conserved residues are highlighted in yellow and polar basic amino acids are indicated in red, blue, and green. Sequence files were retrieved from EXPASY.

similarity in the overlap of lowest energy conformation structures of OTA^- and OTA^{2-} indicates only one docking location in site I is present. The question at hand is the fate of the proton.

Two general reactions can be written to describe the binding of OTA^-.

$$OTA^- + HSA \rightarrow OTA^{2-}/HSA + H^+(solv) \quad (2)$$

$$OTA^- + HSA \rightarrow OTA^{2-}/HSA^+ \quad (3)$$

In reaction 2, the proton released upon binding is taken up by the buffer solution. In reaction 3 the proton remains in the protein.

Two possible scenarios also exist for the binding of the OTA^{2-} from solution.

$$OTA^{2-} + HSA + H^+(solv) \rightarrow OTA^{2-}/HSA^+ \quad (4)$$

$$OTA^{2-} + HSA \rightarrow OTA^{2-}/HSA \quad (5)$$

In reaction 4, a proton is taken up by the protein upon binding of the OTA dianion. In reaction 5, binding does not involve any proton uptake.

Because the binding of MOA to HSA is accompanied by the uptake of a proton from the solvent and MOA and OTA occupy the same binding site, it is reasonable to postulate that the binding of the dianion of OTA will also involve proton uptake. In the case of binding of the monoanion, the proton could be provided by the OTA molecule itself. For the dianion, the proton would need to be taken up from the solvent, similar to that observed for MOA. In this model, the reaction process would be reflected by eqs 3 and 4. These two reactions contribute to ΔH_{app} in accordance with the mole fraction of monoanion and dianion present in solution. If this model is correct, then we expect a plot of ΔH_{app} as a function of ΔH_{buffer} to give a slope of $n_H{}^+ = 0.46$, the mole fraction of the dianion.

The best-fit line from a plot of ΔH_{app} as a function of ΔH_{buffer} (data not shown) reveals a slope of 0.23 ± 0.08 and an intercept (ΔH_{bind}) of -8.06 ± 0.56 kcal/mol. However, the slope in this case corresponds to $\chi_{OTA^-} n_H{}^+$, where χ_{OTA^-} is the mole fraction of OTA^-. At pH 7.13, $\chi_{OTA^-} = 0.54$, so $n_H{}^+ = 0.43 \pm 0.15$, which is consistent with the above expectation ($n_H{}^+ = 0.46$). It is important to consider what would happen if the other binding scenarios (eqs 2 and 5) occurred. If binding of the dianion did not involve proton uptake from the solvent (eq 5), then we would obtain $n_H{}^+ = 0$. If the binding of the monoanion resulted in the release of a proton to the solvent (eq 2), then we would expect $n_H{}^+ = -0.54$. Thus, the data clearly indicate that protonation of an amino acid within site I of the protein accompanies the binding of the OTA dianion.

Because such protonation occurs for both MOA and OTA, it is reasonable to conclude that the resulting ionic interactions play an important role in determining the binding affinity of the ligand. In the case of MOA, this would be the interaction of the lone pair of an oxygen in an ether bond with the protonated side chain on an amino acid; for OTA^{2-} the ligand moiety would be the phenoxide anion. A stronger interaction energy is expected in the case of the phenoxide anion, and this is consistent with, and could be responsible for, the observed differences in the binding affinities of OTA and MOA, which are 5.2×10^6 and 3.0×10^4 M^{-1}, respectively.

Amino Acid Protonation Site. Although the exact molecular details of the association of OTA with HSA remain to be determined, the data presented herein and in recent publications provide important information. In a recent report, we demonstrated that OTA could be displaced from HSA by TIB, indicating they share a common binding site and bind to Sudlow site I within domain II of HSA.[22] Consider the X-ray crystallographic structures of TIB bound to HSA. For the TIB−HSA complex, R257, S287, K199, and H242 are within 5 Å of the ligand.[30] Residues K199 and H242 interact with the COO^- on TIB. Comparison with the warfarin-bound structure shows the heterocylic coumarin moiety of warfarin occupies the same region as the benzyl ring of TIB. Both ligands hydrogen bond to H242 and share the site surrounded by A291, I260, I264, I290, L238, and V241.[30,31] TIB displaces bound OTA and under certain conditions, warfarin may also displace bound OTA.[22,32] The carboxylic acid moiety of TIB interacts with K199 and H242 whereas the O^- substituent of warfarin only interacts with H242.

To account for its displacement by TIB and warfarin, it is reasonable to postulate that the carboxylic group of OTA binds to K199. Given this placement, the isocoumarin ring of OTA would occupy the location near the benzyl moiety of warfarin. If we use the lowest energy conformation of OTA,[33] the phenyl ring would be located in a site lined by F211, W214, L219, and L238. Thus, in principle, residues R257, H242, R222, and R218 could be well-positioned to be involved in the proton transfer from OTA^-. This set of amino acids is also consistent

with the modeling of the OTA binding site reported by McMasters et al.[33]

Examination of albumin amino acid sequences from other species provides additional information because BSA, RSA, and PSA also cause deprotonation of OTA^- upon its binding. Sequence analysis of subdomain IIA (Figure 5) shows that HSA residues H242 and R222, are not conserved. However, R218 and R257 are conserved among these species. We are currently investigating the binding of OTA to recombinant domains with mutations at these residues. Furthermore, we are performing docking experiments with OTA^{2-} to provide more information on electrostatic interactions involved in binding.

Previously, thermodynamic analysis of HSA ligands with varying degrees of acidity indicates the binding of ionizable ligands involves both electrostatic and hydrophobic interactions.[34] The flexibility of the tertiary structure of HSA makes it susceptible to changes in pH, ionic strength, etc. Albumin has an overall net negative charge (−15) due to the large number of charged amino acids, however the charge is distributed asymmetrically about the molecule. The negative charge is highest in domain I (−9), slightly less negative in domain II (−8), and positive in domain III (+2). At physiological pHs, the imidazoles of the histidines are protonated along with terminal amino and carboxylic acids, but all remaining sides chains should maintain a charge.[28]

The protonation equilibrium that takes place between the OTA/HSA complex may have several impacts in OTA toxicity. We have noted beforehand that a protonation step is associated with the entry of OTA into the kidney.[22] This event could affect the transport of the toxin within the nephron or the pH changes that are present within the kidney after exposure to OTA. The stability of the OTA/HSA complex may also contribute to the long half-life and the high affinity of the toxin. In addition, variations in the charge of HSA may play an important role in endocytosis. Electrostatic interactions impact the luminal uptake of proteins that bind to the multiligand receptors (e.g., megalin) as binding is attributed to the interactions of positively charged domains of the protein molecule with the negatively charged domains of megalin.[35] Studies with cationic HSA illustrate an increase in endocytosis of HSA;[36] therefore, a variation in the electrostatics of HSA could impact endocytosis. In fact, OTA has previously been shown to affect albumin endocytosis. Gekle et al. have previously indicated the presence of OTA has reduced the transport capacity and apparent affinity of albumin in opossum kidney cells, and have suggested OTA induced proteinuria may result.[37]

Acknowledgment. This work was supported by Duke University (J.D.S.), National Institute of Health (D.N.B.), and the Alfred Benzon Foundation (E.J.T.).

References and Notes

(1) Van Der Merwe, K. J.; Steyn, P. S.; Fourie, L.; D. B. S.; Theron, J. J. *Nature* **1965**, *205*, 1112−1113.
(2) Van Der Merwe, K. J.; Steyn, P. S.; Fourie, L. *J. Chem. Soc.* **1965**, 7083−7088.
(3) Pohland, A. E.; Nesheim, S.; Friedman, L. *Pure Appl. Chem.* **1992**, *64*, 1029−1046.
(4) Chu, F. S. *Mutation Res.* **1991**, *259*, 291−306.
(5) Galvano, F.; Piva, A.; Ritieni, A.; Galvano, G. *J. Food Prot.* **2001**, *64*, 120−131.
(6) Kuiper-Goodman, T.; Scott, P. M. *Biomed., Environ. Sci.* **1989**, *2*, 179−248.
(7) Kuiper-Goodman, T. *Food Addit., Contam.* **1996**, *13*, 53−57.
(8) Petzinger, E.; Ziegler, K. *J. Vet. Pharmacol. Ther.* **2000**, *23*, 91−98.
(9) Studer-Rohr, I.; Schlatter, J.; Dietrich, D. R. *Arch. Toxicol.* **2000**, *74*, 499−510.
(10) Purchase, I. F.; Van der Watt, J. J. *Food Cosmet. Toxicol.* **1971**, *9*, 681−2.
(11) Eder, S.; Benesic, A.; Freudinger, R.; Engert, J.; Schwerdt, G.; Drumm, K.; Gekle, M. *Pflugers Arch.* **2000**, *440*, 521−529.
(12) Gekle, M.; Pollock, C. A.; Silbernagl, S. *J. Pharmacol. Exp. Ther.* **1995**, *275*, 397−404.
(13) Kuramochi, G.; Gekle, M.; Silbernagl, S. *Eur. J. Physiol.* **1997**, *434*, 392−7.
(14) Schwerdt, G.; Freudinger, R.; Silbernagl, S.; Gekle, M. *Toxicology* **1998**, *131*, 193−202.
(15) Schwerdt, G.; Gekle, M.; Freudinger, R.; Mildenberger, S.; Silbernagl, S. *Biochim. Biophys. Acta* **1997**, *1324*, 191−9.
(16) Galtier, P. Etude toxicologique et pharmacocinetique d'une mycotoxine, l'ochratoxine A., Toulouse, 1979.
(17) Galtier, P.; Alvinerie, M.; Charpenteau, J. L. *Food Chem. Toxicol.* **1981**, *19*, 735−738.
(18) Chu, F. S. *Arch. Biochem. Biophys.* **1971**, *147*, 359−366.
(19) Il'ichev, Y. V.; Perry, J. L.; Simon, J. D. *J. Phys. Chem. B* **2002**, *106*, 452−459.
(20) Uchiyama, S.; Saito, Y.; Uchiyama, M. *J. Food Hyg. Soc. Jpn.* **1985**, *26*, 651−657.
(21) Uchiyama, S.; Saito, Y. *J. Food Hyg. Soc. Jpn.* **1987**, *28*, 453−460.
(22) Il'ichev, Y. V.; Perry, J. L.; Rüker, F.; Dockal, M.; Simon, J. D. *Chem. Bio. Inter.* **2002**, *141*, 275−293.
(23) Perry, J. L.; Il'ichev, Y. V.; Kempf, V. R.; McClendon, J.; Park, G.; Manderville, R. A.; Rüker, F.; Dockal, M.; Simon, J. D. *J. Phys. Chem. B*, in press.
(24) Xiao, H.; Marquardt, R. R.; Frohlich, A. A.; Ling, Y. Z. *J. Agric. Food Chem.* **1995**, *43*, 524−530.
(25) Wiseman, T.; Williston, S.; Brands, J. F.; Lin, L. N. *Anal. Biochem.* **1989**, *179*, 131−137.
(26) Leavitt, S.; Freire, E. *Curr. Opin. Struct. Biol.* **2001**, *11*, 560−566.
(27) Goldberg, R. N.; Kishore, N.; Lennen, R. M. *J. Phys. Chem. Ref. Data* **2001**, *30*, 1−140.
(28) Peters, T. *All About Albumin*; Academic Press: New York, 1996.
(29) Kasai-Morita, S.; Horie, T.; Awazu, S. *Biochim. Biophys. Acta* **1987**, *915*, 277−283.
(30) Curry, S.; Mandelkow, H.; Brick, P.; Franks, N. P. *Nature Struct. Biol.* **1998**, *5*, 827−835.
(31) Petitpas, I.; Bhattacharya, A. A.; Twine, S.; East, M.; Curry, S. *J. Biol. Chem.* **2001**, *276*, 22804−22809.
(32) Il'ichev, Y. V.; Perry, J. L.; Simon, J. D. *J. Phys. Chem. B* **2002**, *106*, 460−465.
(33) McMasters, D. R.; Vedani, A. *J. Med. Chem.* **1999**, *42*, 3075−86.
(34) Urien, S.; Nguyen, P.; Berlioz, S.; Bree, F.; Vacherot, F.; Tillement, J. P. *Biochem. J.* **1994**, *302*, 69−72.
(35) *The Kidney Physiology and Pathophysiology*, 3rd ed.; Seldin, D. W., Giebisch, G., Eds.; Philadelphia, 2000.
(36) Parks. *J. Clin. Invest.* **1984**, *73*, 767−777.
(37) Gekle, M.; Mildenberger, S.; Freudinger, R.; Silbernagl, S. *J. Pharmacol. Exp. Ther.* **1994**, *271*, 1−6.